Dynamic model of a plasma structure with an intermediate double-layer, formed outside an anodic plasma contactor

V. Lapuerta and E. Ahedo[a)]
E.T.S.I. Aeronáuticos, Universidad Politécnica, Madrid, Spain

(Received 3 August 1999; accepted 16 February 2000)

The plasma structure around an electron-collecting, plasma contactor consists of two quasineutral regions separated by an intermediate, free double layer(DL). A dynamic model of this three-region structure is here established, based in a linear perturbation of the complete steady solution. Time-dependent conditions at the mobile DL are obtained; these consist of Bohm and Langmuir laws, jump conditions on the accelerated species and barrier conditions on the confined ones. Boundary conditions at the contactor surface and at the undisturbed, ambient plasma are analyzed in detail. The dynamic response to perturbations in plasma emission is the combination of a quasisteady electron mode and several ion–electron modes, with different characteristics in the core and presheath. Mode interaction takes place through the DL and the electric potential. At large frequencies, the DL displacement is restricted by ambient ions, which tend to be rigid. The stability of the steady solution is studied through a nonlocal dispersion relation. It is found that this plasma structure does not develop the radial, ion–electron (macro)instability, and, in particular, the Buneman instability. © *2000 American Institute of Physics.* [S1070-664X(00)01206-4]

I. INTRODUCTION

An electron-collecting (anodic) contactor is a device biased positively with respect to an external plasma, that discharges an internally produced plasma into the ambient plasma. In an unmagnetized environment and within the convenient ranges of plasma emission and bias voltage, the structure of the plasma outside the contactor consists of two quasineutral regions (core and presheath) separated by a space-charge, double layer(DL) where most of the potential drop takes place,[1–3] Figs. 1(a) and 1(b). The DL acts then as an acceleration layer for one species from each plasma, and as a confining wall for the other plasma species (this kind of double layers are named ''strong,'' generally). The experimental evidence is that these structures with DLs are easily sustained during a long time, but, at the same time, Williams and Wilbur[1] report a significant level of fluctuations (up to a 60%). Anomalous plasma heating, possibly related to a weakly turbulent state, was also detected by Vannaroni *et al.*[2] Structures with intermediate DLs are not exclusive of plasma contactor plumes; for an extensive review of DL phenomena see the papers of Hershkowitz[4] and Raadu.[5] Several experiments (in double and triple plasma chambers mainly) where fluctuations at both low(ion) and high(electron) frequencies coexist with an apparently ''stable'' DL structure, are commented in these reviews.

Plasma acceleration by the strong electric field of the DL creates two counter-streaming, high-energy beams in the two quasineutral regions. This points to saturated, current-driven instabilities as the most probable cause of the observed weakly turbulent state. However, the exact nature of the instability for each experimental situation is controversial, and the interaction between the average and the fluctuating modes in the final, stable state is not well known. For the plasma contactor case, Vannaroni *et al.*[2] discussed the presence of the ion–acoustic and bump-in-tail instabilities and concluded that the second one could explain the anomalous heating observed in their experiments. Other papers[6–8] have proposed the simultaneous development in the plasma plume of the Buneman and ion–acoustic instabilities, which are two limit cases of the ion–electron instability.[9] Two of these papers[6,7] even discussed the final turbulent state with a steady model that included effective collision terms for the two saturated instabilities. The consistency of this model is quite uncertain: First, the choice of the two instability modes is not well supported, since there is no analysis of the dynamic response of the global plasma structure; and second, the expressions they used for the collision terms were taken from studies of infinite, homogeneous, two-species plasmas. These last attributes are certainly not applicable to the plasma in the core. The simplest, plausible model of the core must include two electron species, which means more involved and varied interactions (ion–electron, electron–electron). Furthermore, the core dynamic response is coupled with the DL displacement and the dynamic response in the presheath, which is itself constituted by a different three-species plasma.

The dynamic behavior of plasma structures with an internal DL has been studied mainly through numerical simulations.[4,5] Most of them consider a plasma configuration appropriate for a triple-plasma machine: a finite, planar domain with two electrodes at the boundaries, that emit and collect plasma. An external circuit between the two electrodes is often included to preserve charge conservation. In contrast to experiments, the double layers created in these planar simulations are never stable. The simulation of the

[a)]Electronic mail: ahedo@fmetsia.upm.es

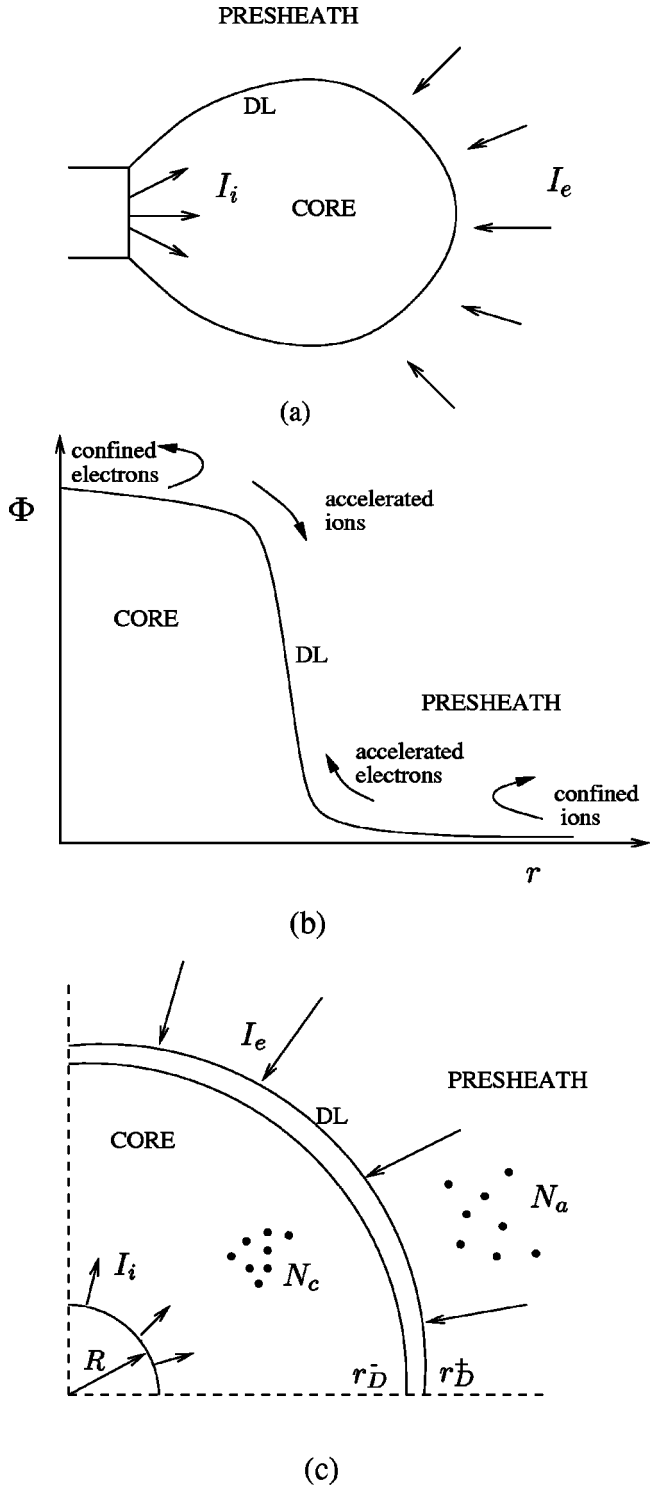

FIG. 1. (a) Sketch of a typical plasma structure with intermediate DL found in experiments. (b) Typical, axial profile of the electric potential and its effect on the four plasma species. (c) Spherical model of the plasma structure used in this paper.

plasma configuration around a contactor is even harder, because of the nonplanar geometry, more inhomogeneous plasma profiles, and the need to simulate the ambient, undisturbed plasma. Marshall and Neubauer[10] tried this problem and only obtained solutions with strong fluctuations and no DL. Hubbard and Joyce[11] have pointed out that the problems in the simulations come mainly from the boundary conditions, which (i) are not periodical, (ii) must preserve the global electrical neutrality, and (iii) must simulate two counterstreaming flows and the injection of particles of the confined species. The consequence is that the dynamic behavior is affected by undesirable wave reflections at the boundaries and artificial coupling between plasma conditions at both electrodes.

In view of the difficulties encountered by numerical simulations to reproduce a fully nonlinear, time-dependent solution, this paper proposes an analytical approach of the contactor problem based in a time-dependent, linear perturbation of a well-defined steady solution. This perturbation model will clarify fundamental aspects of the dynamic response, like (i) the temporal modes that propagate in the multispecies plasmas at both DL sides, (ii) the boundary conditions at the contactor surface and at the ambient plasma, (iii) the transition and jump conditions at the mobile DL, and (iv) the instability types that may develop in the global structure. The understanding of these points is an adequate basis for a consistent formulation of a steady, weakly turbulent model and for a correct design of numerical simulations.

For the dynamic model to be investigated analytically we consider a simplified formulation, consisting of macroscopic plasma equations and a spherical geometry, Fig. 1(c). A fully macroscopic, dynamic version of the (partially kinetic) model of Ahedo, Sanmartín, and Martínez-Sánchez[12] is used. This model determines completely the parameters and spatial profiles of the steady solution (including the transition conditions to the DL), which is essential to apply consistently the perturbation techniques. The model of Ahedo *et al.* neglects collisions with neutrals in the plasma plume. A later model of Ahedo,[13] which includes external ionization due to electron–neutral collisions, could not be used here because a fully macroscopic formulation of it is not completed yet.

For a spatially nonuniform solution, the temporal perturbation theory determines the spatial profile for each individual mode of (complex) frequency Ω. The analysis here will contemplate both the response to a time-dependent plasma emission and the (absolute) instability behavior of the steady solution, excepting kinetic (or micro-) instabilities that cannot be analyzed with a macroscopic model. Due to the dissimilar characteristic times of response of ions and electrons, there are, at least, two distinguished ranges of frequencies, with rather different plasma dynamics. In this paper, the discussion is restricted to low-frequency modes, dominated by ion dynamics.

The paper is organized as follows. Section II details the hypotheses and equations that constitute the time-dependent model, and analyzes the quasisteady equations of a thin, free DL. Section III briefly summarizes the parameters and conditions that define the steady presheath/DL/core solution. Section IV formulates the perturbation model, with special attention to conditions at the DL. Section V completes the details of the perturbation model in each region and defines the procedure for the numerical integration; an asymptotic solution for large ion frequencies is presented, also. Section VI has two subsections: The first one studies the regular plasma response to a time-dependent plasma emission; and

the second one discusses the nonexistence of a radial, ion–electron macroinstability, in particular of the Buneman instability. Section VII collects final comments and extensions of the present work.

II. FORMULATION OF THE MODEL

A spherically symmetric model is considered with r and t as the radial and temporal variables. The contactor is a sphere of radius R which emits an artificial plasma into a quiescent, unmagnetized plasma, Fig. 1(c). The undisturbed density and temperature of the ambient plasma are N_∞ and T_∞, respectively. The contactor is biased to a potential $\Phi(R,t)$ positive and large compared to the mean plasma temperature. Hence, ions from the ambient plasma (species a) are prevented from approaching the contactor, while ambient electrons (species e) are accelerated inwards and, part of them, collected by the contactor; let $I_e(t)$ be the electron current collected by the contactor. The artificial plasma is characterized by the current $I_i(t)$ of emitted ions (species i), which are accelerated outwards, and by the equilibrium temperature T_c of emitted electrons (species c), which remain confined around the contactor. The emitted current $I_i(t)$ is assumed large enough to sustain a plasma structure consisting of (i) a quasineutral plasma cloud (the *core*) surrounding the contactor, (ii) a space-charge *double layer*, where most of the potential drop takes place, and (iii) an exterior quasineutral region (the *presheath*). The ratio $\lambda_{D\infty}/R$, with $\lambda_{D\infty}=(\epsilon_0 T_e/e^2 N_\infty)^{1/2}$, is considered small enough to adopt a two-scale analysis, where the DL is treated as a free discontinuity in the quasineutral scale (related to R). The thickness Δr_D of a quasiplanar, strong DL verifies[5]

$$\Delta r_D \sim \lambda_{D\infty}(e\Delta\Phi_D/T_\infty)^{3/4} \ll r_D,$$

where $r=r_D(t)$ is the DL position and $\Delta\Phi_D=\Phi(r_D^-)-\Phi(r_D^+)$ is the potential jump across the DL. The plasma/contactor model must determine $I_e(t)$, $r_D(t)$, $\Phi(r_D^-,t)$, $\Phi(r_D^+,t)$, and the plasma profiles in terms of $\Phi(R,t)$, $I_i(t)$, and the rest of plasma parameters. The dynamic model developed here considers the plasma response to small, dynamic perturbations of the steady solution, in particular those produced by an unsteady plasma emission,

$$I_i(t)=I_{i0}+I_{i1}(t),\quad I_{i1}\ll I_{i0}.$$

The dynamic response is obtained as sum of the steady solution and the dynamic solution of the linear perturbation problem; subscripts 0 and 1 are used throughout the paper for these two solutions, respectively.

The dynamics of the four plasma species is represented by the following macroscopic equations:

$$\frac{\partial N_\alpha}{\partial t}+\frac{\partial}{\partial r}(N_\alpha V_\alpha)=0,$$

$$m_\alpha\frac{\partial V_\alpha}{\partial t}+m_\alpha V_\alpha\frac{\partial V_\alpha}{\partial r}+\frac{1}{N_\alpha}\frac{\partial N_\alpha T_\alpha}{\partial r}+q_\alpha\frac{\partial\Phi}{\partial r}=0, \qquad (1)$$

$$T_\alpha N_\alpha^{1-\varrho_\alpha}=\text{const},$$

where $\alpha=i,e,a,c$ is representing each species, V_α are macroscopic velocities, N_α are densities, T_α are temperatures, m_α are particle masses, $q_\alpha=\pm e$ are electric charges (and all ions are assumed singly charged), and ϱ_α are heat specific ratios (equal to three for free species i and e, and one for confined species, a and c, according to Ref. 12). Collisions among the different plasma species and with neutrals are not included in this model. Poisson equation for the electrostatic potential

$$\frac{\varepsilon_0}{r^2}\frac{\partial}{\partial r}\left(r^2\frac{\partial\Phi}{\partial r}\right)=-\sum_\alpha q_\alpha N_\alpha, \qquad (2)$$

closes the set of Eq. (1); it simplifies to the quasineutral condition $\Sigma q_\alpha N_\alpha\simeq 0$, in core and presheath. These two regions are matched through the jump conditions across the DL discontinuity, which are obtained from the DL internal equations.

A. Quasisteady model of the double layer

Plasma equations inside a quasiplanar DL admit a simple formulation. First, in a reference frame tied to the DL, the plasma motion is quasisteady (except for very large frequency modes, not considered in this paper) and verifies

$$N_\alpha\tilde{V}_\alpha\simeq\text{const},$$
$$m_\alpha\tilde{V}_\alpha^2/2+H_\alpha+q_\alpha\Phi\simeq\text{const}, \qquad (3)$$

where $\tilde{V}_\alpha=V_\alpha-dr_D/dt$ are velocities in the DL frame, $H_\alpha=\varrho_\alpha T_\alpha/(\varrho_\alpha-1)+\text{const}$, for free species, and $H_\alpha=T_\alpha\ln N_\alpha+\text{const}$, for confined species. Second, Eq. (2) simplifies to its quasiplanar form, which, using Eq. (3), yields the integral law

$$\frac{\varepsilon_0}{2}\left(\frac{d\Phi}{dr}\right)^2-S(\Phi)\simeq\text{const},\quad S=\sum_\alpha\left(m_\alpha N_\alpha\tilde{V}_\alpha^2+N_\alpha T_\alpha\right). \qquad (4)$$

This is the equation of conservation of momentum of the whole plasma, and states the equilibrium between the pressure of the electric field and the stagnation pressure of the plasma; $S(\Phi)$ is normally termed the Sagdeev potential.

Constants in Eqs. (3) and (4) are determined from the matching between the two quasineutral regions and the DL. The ratio between the electric fields outside and inside the DL is $\lambda_{D\infty}/r_D\ll 1$, so this two-scale analysis may consider that $\lambda_{D\infty}d(\ln\Phi)/dr\to 0$ at r_D^- and r_D^+. Then, the constant of Eq. (4) is

$$S(\Phi_D^+)=S(\Phi_D^-). \qquad (5)$$

This equality is also the expression of Langmuir condition, which states both that the plasma pressure at both DL sides is the same, and the total electric charge of the DL is zero. More generally, the Sagdeev potential inside the DL must satisfy

$$S(\Phi)-S(\Phi_D^-)=S(\Phi)-S(\Phi_D^+)>0. \qquad (6)$$

Then, from Taylor expansion of the left-hand sides of Eq. (6), and since $S'(\Phi_D^\pm)=-\Sigma q_\alpha N_\alpha(\Phi_D^\pm)=0$, a transition from a quasineutral plasma to a DL requires that

$$S''(\Phi_D^\pm)>0,\ \text{or}\ [S''(\Phi_D^\pm)=0\ \text{and}\ S'''(\Phi_D^\pm)\neq 0], \qquad (7)$$

which are the regular and singular forms, respectively, of Bohm condition.

Once constants in Eqs. (3) and (4) are set, plasma profiles inside the DL are obtained by integrating Eq. (4). This integration is straightforward when $S(\Phi)$ is a one-branch function. Furthermore, only Langmuir and Bohm conditions are then needed to solve the response of the quasineutral plasma.

III. STEADY SOLUTION

A brief derivation of the steady solution of Ahedo *et al.* is presented here, with emphasis on the aspects that are relevant for the perturbation problem, like transitions to the DL, boundary conditions at the contactor, and dimensionless parameters that define the response. Subjects like the uniqueness of the solution and the orbital-motion-limit regime, are omitted.

For steady boundary conditions, the steady solution (denoted with subscript 0) verifies the set of conservation equations

$$r^2 N_{e0} V_{e0} = \text{const} = J_{e0}, \tag{8}$$

$$m_e V_{e0}^2/2 - e\Phi_0 + 3T_{e0}/2 = 3T_\infty/2, \tag{9}$$

$$T_{e0}/T_\infty = N_{e0}^2/N_\infty^2, \tag{10}$$

$$r^2 N_{i0} V_{i0} = \text{const} = J_{i0}, \tag{11}$$

$$m_i V_{i0}^2/2 + e\Phi_0 + 3T_{i0}/2 = \text{const} = K_{i0R}, \tag{12}$$

$$T_{i0}/T_{i0R} = N_{i0}^2/N_{i0R}^2, \tag{13}$$

$$N_{a0} = N_\infty \exp(-e\Phi_0/T_\infty), \quad r > r_{D0}, \tag{14}$$

$$N_{c0} = N_{c0R} \exp\left(e\frac{\Phi_0 - \Phi_{0R}}{T_{c0}}\right), \quad r < r_{D0}, \tag{15}$$

where: Subscript R refers to $r=R$; $J_{e0}(<0)$ and J_{i0} are the particle flows of the two free species; and the restriction of each confined species to just one side of the strong DL is consistent with the macroscopic model and simplifies the treatment of the quasineutral model. In the core and presheath, the quasineutral condition

$$N_{i0} + N_{a0} - N_{e0} - N_{c0} \simeq 0, \tag{16}$$

is added to close the problem. Equations (8)–(16) define implicitly the spatial profiles of $\Phi_0(r)$ and the rest of the plasma variables. For the desired range of parameters this solution presents turning points with $d/dr = \pm\infty$, which must denote either a transition to a space-charge layer or the contactor surface. For instance, the electric field verifies

$$\frac{d\Phi_0}{dr} = \frac{2}{r}\frac{Q_0}{P_0}, \quad P_0 = \sum_\alpha \frac{q_\alpha^2 N_{\alpha 0}}{\varrho_\alpha T_{\alpha 0} - m_\alpha V_{\alpha 0}^2},$$
$$Q_0 = -\sum_\alpha \frac{q_\alpha N_{\alpha 0} m_\alpha V_{\alpha 0}^2}{\varrho_\alpha T_{\alpha 0} - m_\alpha V_{\alpha 0}^2}, \tag{17}$$

so turning (singular) points of the quasineutral solution correspond to

$$P_0 = 0. \tag{18}$$

It is easily seen that P_0 is the second derivative of Sagdeev potential, S_0'', so Eq. (18) is the Bohm singular condition. The transition point, $r = r_{D0}^+$, from presheath to DL is one of the solutions of this equation [no valid solution of the DL has been found with $P_0(r_{D0}^+) > 0$]. The DL–core transition point, $r = r_{D0}^-$, is obtained from Langmuir condition (5), which here takes the form

$$\left[\sum_\alpha (m_\alpha N_{\alpha 0} V_{\alpha 0}^2 + N_{\alpha 0} T_{\alpha 0})\right]_{r_{D0}^-}^{r_{D0}^+} = 0.$$

It comes out that, contrary to r_{D0}^+, the transition from DL to core is a regular point with $P_0(r_{D0}^-) > 0$, so a regular solution in the core requires P_0 to be positive for $R < r < r_{D0}^-$. Since, in a loose sense, condition $P_0 = 0$ is related to ''sonic'' conditions of the emitted plasma,[12] $P_0(R) = 0$ will be imposed unless stated otherwise. This eliminates the ion velocity at the contactor exhaust, V_{i0R}, as a free parameter. Also, it was justified by Ahedo *et al.* that, since the emitted ions flow sonic/supersonically, T_{i0} affects the solution weakly and can be neglected.

With respect to the formulation presented here the model discussed in Ref. 12 makes two additional hypotheses that restrict the parametric range of validity of the solution. First, it disregards thermal effects of the attracted electrons in the core, which is valid while the core size is not very large. Second, it neglects the influence of the emitted ions in the presheath solution, which is valid for large contactor potentials ($e\Phi_{0R}/T_\infty > 10^2$, roughly). The two restrictions will be kept here; only the second one may have some influence on the low-frequency response, as will be commented later.

For a compact representation of the solution, R, N_∞, and T_∞ are used to define nondimensional variables and parameters:

$$\xi = \frac{r}{R}, \quad \phi = \frac{e\Phi}{T_\infty}, \quad t_\alpha = \frac{T_\alpha}{T_\infty}, \quad n_\alpha = \frac{N_\alpha}{N_\infty},$$
$$v_\alpha = \frac{V_\alpha}{(T_\infty/m_\alpha)^{1/2}}, \quad j_\alpha = \frac{J_\alpha}{R^2 N_\infty (T_\infty/m_\alpha)^{1/2}}.$$

Using this nondimensionalization, the steady solution depends on three parameters; in particular, the C-V characteristic takes the form $j_{e0} = j_{e0}(j_{i0}, \phi_{0R}, t_{c0})$. Figure 2 shows examples of the C-V response and steady plasma profiles.

IV. PERTURBATION MODEL

A generic variable or parameter, let us say f, is decomposed as

$$f(r,t) \simeq f_0(r) + f_1(r,t),$$
$$f_1(r,t) = (2\pi)^{-1} \int_L f_1(r,\Omega) \exp(-i\Omega t) d\Omega, \tag{19}$$

where $f_0(r)$ is the steady part, $f_1(r,t)$ is the time-dependent perturbation, $f_1(r,\Omega)$ is its Laplace transform, $\Omega = \Omega_{re} + i\Omega_{im}$ is a complex frequency and L is the Laplace integra-

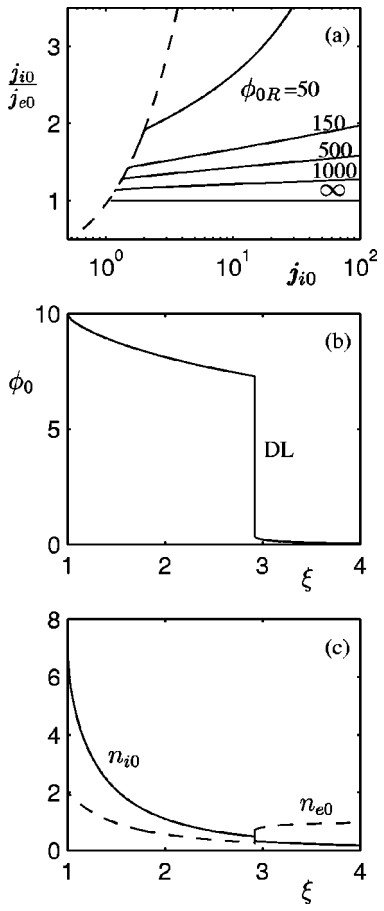

FIG. 2. Steady solution: (a) Current-voltage response, $j_{e0}(j_{i0},\phi_{0R})$, for $t_{c0}=10$; the dashed line corresponds to $\xi_{D0}=1$, the transition to the no-core solution. (b) and (c) Spatial profile of the electric potential and the densities of the two free species for $\phi_{0R}=10$, $j_{i0}=14.3$, and $t_{c0}=1$; $\xi=\xi_{D0}^{+}$ and $\xi=1$ are singular points of the quasineutral equations; $n_{i0}-n_{e0}$ is equal to n_{c0} in the core and to $-n_{a0}$ in the presheath.

tion path. Modes are purely oscillatory (in time) when Ω is real, and purely monotonic when $i\Omega$ is real. The designation of ''acoustic'' and ''standing'' modes, natural for Ω real, will be employed here for any Ω, whether real or complex.

To facilitate the mathematical treatment of the perturbation equations, the perturbed particle flow and mechanical energy,

$$J_{\alpha 1}=r^2(N_{\alpha 1}V_{\alpha 0}+N_{\alpha 0}V_{\alpha 1}),$$
$$K_{\alpha 1}=m_\alpha V_{\alpha 0}V_{\alpha 1}+\varrho_\alpha T_{\alpha 0}N_{\alpha 1}/N_{\alpha 0}+q_\alpha\Phi_1, \tag{20}$$

respectively, will be used as perturbation variables, instead of $N_{\alpha 1}$ and $V_{\alpha 1}$. Applying expansion (19) to Eq. (1), the perturbation equations for each plasma species and each Ω-mode are

$$dJ_{\alpha 1}/dr-i\Omega r^2N_{\alpha 1}=0,$$
$$dK_{\alpha 1}/dr-i\Omega m_\alpha V_{\alpha 1}=0, \tag{21}$$

with

$$\frac{N_{\alpha 1}}{N_{\alpha 0}}=\frac{K_{\alpha 1}-q_\alpha\Phi_1-m_\alpha V_{\alpha 0}^2J_{\alpha 1}/J_{\alpha 0}}{\varrho_\alpha T_{\alpha 0}-m_\alpha V_{\alpha 0}^2},$$
$$\frac{V_{\alpha 1}}{V_{\alpha 0}}=\frac{-K_{\alpha 1}+q_\alpha\Phi_1-\varrho_\alpha T_{\alpha 0}J_{\alpha 1}/J_{\alpha 0}}{\varrho_\alpha T_{\alpha 0}-m_\alpha V_{\alpha 0}^2}, \tag{22}$$

obtained from (20). In the core and presheath, these equations are completed with $\Sigma q_\alpha N_{\alpha 1}\simeq 0$. Substituting here $N_{\alpha 1}$ from Eq. (22), the perturbed electric potential Φ_1 is obtained as a linear combination of $J_{\alpha 1}$ and $K_{\alpha 1}$

$$\Phi_1=\frac{Q_1}{P_0},\quad Q_1=\sum_\alpha q_\alpha N_{\alpha 0}\frac{K_{\alpha 1}-m_\alpha V_{\alpha 0}^2J_{\alpha 1}/J_{\alpha 0}}{\varrho_\alpha T_{\alpha 0}-m_\alpha V_{\alpha 0}^2}, \tag{23}$$

with P_0 defined in Eq. (17). Equations (21)–(23) form a closed set for the two quasineutral regions.

Plasma perturbations produce a displacement, $r_{D1}(t)=r_D(t)-r_{D0}$, of the free DL from its position in the steady solution, which must be determined. Because of this displacement and in order to represent the dynamic response (zeroth plus first-order solutions) the spatial variable r needs to be stretched with the linear change $r\to s(r,t)$

$$\frac{s-r_{D0}}{r-r_D(t)}=\begin{cases}\dfrac{r_{D0}-R}{r_D(t)-R}, & \text{for } r<r_D\\ 1, & \text{for } r>r_D\end{cases}, \tag{24}$$

which transforms $r=R$ and $r=r_D(t)$ into $s=R$ and $s=r_{D0}$, respectively. Once solutions $f_0(r)$ and $f_1(r,t)$ are known, the total response of f at $s=s^*$ and any t is (neglecting nonlinear contributions)

$$f(r(s^*,t),t)\simeq f_0(s^*)+\hat f_1(s^*,t),$$
$$\hat f_1(s^*,t)=f_1(s^*,t)+[r(s^*,t)-s^*]\frac{df_0}{dr}(s^*).$$

In particular, the total perturbation at each DL side is $\hat f_1(r_{D0}^{\pm},t)$, and the DL jump conditions of the perturbation problem, derived from Eqs. (3) and (4), are

$$[J_{\alpha 1}+i\Omega r_{D1}r_{D0}^2N_{\alpha 0}]_{r_{D0}^-}^{r_{D0}^+}=0,$$
$$[K_{\alpha 1}+i\Omega r_{D1}m_\alpha V_{\alpha 0}]_{r_{D0}^-}^{r_{D0}^+}=0, \tag{25}$$
$$\sum_\alpha\Big[2m_\alpha N_{\alpha 0}V_{\alpha 0}(V_{\alpha 1}+i\Omega r_{D1})+m_\alpha N_{\alpha 1}V_{\alpha 0}^2+\varrho_\alpha N_{\alpha 1}T_{\alpha 0}$$
$$+r_{D1}\frac{d}{dr}(m_\alpha N_{\alpha 0}V_{\alpha 0}^2+N_{\alpha 0}T_{\alpha 0})\Big]_{r_{D0}^-}^{r_{D0}^+}=0,$$

where the Laplace transform and zeroth-order jump conditions have already been applied, and $i\Omega r_{D1}$ is the displacement velocity of the DL. The last equation is the perturbation of the Langmuir condition.

The temporal response of ions and electrons is very different due to their dissimilar masses. Then, there are, at least, two distinguished ranges for the frequency of the perturbation modes: *Ion frequencies*, $\Omega\sim R^{-1}\sqrt{T_\infty/m_i}$, when the

electron response is quasisteady, and plasma dynamics are based in ion–electron modes; and *electron frequencies*, $\Omega \sim R^{-1}\sqrt{T_\infty/m_e}$, when ions stay rigid in their stationary response, and plasma dynamics are dominated by electron–electron modes and, perhaps, space-charge modes. Each frequency range has its own set of equations and boundary conditions, if variables are nondimensionalized adequately. For modes in the ion frequency range, the convenient dimensionless frequency is

$$\omega = \Omega R/\sqrt{T_\infty/m_i},$$

with $\omega = O(1)$ as the distinguished case, and the temporal derivatives are eliminated from electron equations when the asymptotic limit $m_e/m_i \to 0$ is taken.

Boundary conditions of the perturbation problem in the core and presheath consists of: (i) No perturbations of the ambient plasma at $r=\infty$; (ii) the dynamic solution is bounded at any point; (iii) jump condition (25) at the DL are satisfied; (iv) perturbations on conditions at the contactor exhaust are specified. For ion frequency modes, the perturbation of the plasma emission, $J_{i1}(R,t) = I_{i1}(t)/4\pi e$, is the most relevant one.

V. INTEGRATION OF THE PERTURBATION PROBLEM

Like the zeroth-order problem, the perturbation equations are integrated from $\xi=\infty$ to $\xi=1$. The presheath problem, for a steady solution with $n_i \ll n_e$, consists of relations

$$\begin{aligned} &n_{a1} \simeq n_{e1}, \quad j_{e1} = \text{const}, \quad k_{e1} = 0, \\ &\phi_1 = \frac{q_1}{p_0} = \frac{v_{e0}^2 j_{e1}/j_{e0} - (v_{e0}^2 - 3t_{e0})k_{a1}}{1 + 3t_{e0} - v_{e0}^2}, \end{aligned} \tag{26}$$

and two differential equations for the dynamics of ambient ions

$$\begin{aligned} &\frac{1}{\xi^2}\frac{dj_{a1}}{d\xi} - \mathrm{i}\omega_a n_{e0}\frac{k_{a1} - v_{e0}^2 j_{e1}/j_{e0}}{1 + 3t_{e0} - v_{e0}^2} = 0, \\ &\frac{dk_{a1}}{d\xi} - \mathrm{i}\omega_a \frac{j_{a1}}{\xi^2 n_{e0}} = 0. \end{aligned} \tag{27}$$

In Eqs. (26) and (27): $k_{\alpha 1}$, p_0, and q_1 are the dimensionless counterparts of their corresponding capital case variable, Eqs. (20)–(23); $\omega_a = \omega\sqrt{m_a/m_i}$ is used for convenience when ambient and emitted ions are different; and zero perturbation of the ambient plasma at $r=\infty$ has been assumed. Notice that $j_{e1} \neq 0$ is compatible with $n_{e1} = v_{e1} = 0$ at $r=\infty$.

The general solution of Eq. (27) is a linear combination of three modes, and boundary conditions are imposed at $\xi=\infty$ and $\xi = \xi_{D0}^+$. Taking into account the temporal dependence: $\exp(-\mathrm{i}\Omega t)$, the asymptotic behavior for $\omega_a \xi_{D0} \gg 1$ (see next Subsection for a detailed derivation) shows that there are one quasisteady mode, proportional to j_{e1}, and two ion–acoustic modes. Disregarding the acoustic mode that travel inwards (when $\omega_{\mathrm{re}} \neq 0$) and is unbounded at $\xi=\infty$ (when $\omega_{\mathrm{im}} \neq 0$), the asymptotic solution of Eq. (27) at $\xi \gg \xi_{D0}, |\omega_a|^{-1/5}$ is

$$j_{a1}(\xi) \simeq j_{e1}\left[\frac{4\mathrm{i}j_{e0}^2}{\omega_a \xi^5} + \cdots\right] + a_\infty\left[\frac{1}{2\xi}\exp\left(\frac{\mathrm{i}\omega_a}{2}\xi\right) + \cdots\right]. \tag{28}$$

Next, two conditions are imposed at the presheath/DL boundary. First, the DL is a barrier for the ambient ions, so their relative velocity there is zero,

$$\xi = \xi_{D0}^+: \quad j_{a1}/\xi^2 n_{e0} + \mathrm{i}\omega_a \xi_{D1} = 0. \tag{29}$$

Second, since ξ_{D0}^+ is a singular point with $p_0(\xi_{D0}^+) = 0$, the solution must be bounded there. From the expression for the electric potential one has

$$\hat{\phi}_1 = (q_1 + 2q_0\xi_{D1}/\xi_{D0})/p_0,$$

(with $q_0 \equiv Q_0/eN_\infty$), so the numerator in the right-hand side must be zero at $\xi = \xi_{D0}^+$. Substituting q_0 and q_1, this condition becomes

$$\xi = \xi_{D0}^+: \quad v_{e0}^2(j_{e1}/j_{e0} - 2\xi_{D1}/\xi_{D0}) - k_{a1} = 0. \tag{30}$$

It can be shown that Eq. (30) is equivalent to the Bohm singular condition (7) of the perturbation problem: $\hat{S}_1''(r_{D0}^+) = 0$. Conditions (28)–(30) include three parameters: ξ_{D1}, j_{e1}, and a_∞. Thus, for each ω, the integration of Eqs. (26) and (27) yields two relations between these parameters. Therefore, the perturbation solution in the presheath is universal and proportional to one parameter; the most convenient one is j_{e1}.

The numerical integration of the presheath equations presents two problems. The first one is the singularity at $\xi = \xi_{D0}^+$. The change of independent variable $\xi \to \int d\xi/p_0$ makes the equations regular and the numerical integration straightforward. The second problem is harder to solve. In principle, to avoid the unbounded (or out-traveling) mode at $\xi=\infty$, the integration should proceed from $\xi=\infty$ with the two independent modes of the asymptotic solution (28) as ''initial'' conditions. However, their different growth scale makes this procedure impracticable. We were thus forced to integrate from $\xi = \xi_{D0}^+$ and to use an iterative scheme to match with the asymptotic solution at $\xi \gg \xi_{D0}$. The numerical integration from ξ_{D0}^+ with conditions (29) and (30) yields a solution that is the combination of two independent modes, each one proportional to j_{e1} and ξ_{D1}. The correct matching with the asymptotic solution must provide the correct value of j_{e1}/ξ_{D1}. In each iteration step, the solution is built up with two independent modes, each one with a ratio ξ_{D1}/j_{e1} close to a predetermined value. This numerical solution is stopped before the explosive modes develop, at $\xi = \xi_*$ say, and is matched there to the asymptotic solution. This determines the value of ξ_{D1}/j_{e1} to be used in the next iteration step. As the values of ξ_{D1}/j_{e1} are closer to the correct one, the numerical solution can proceed farther. The iteration finishes when the matching point ξ_* is within the admissible interval of the asymptotic solution.

The core problem for species *e*, *c*, and *i* consists of the quasisteady equations for electrons

$$j_{e1} = j_{e1}(\xi_{D0}^+), \quad k_{e1} = 0, \quad j_{c1} = 0, \quad k_{c1} = 0, \tag{31}$$

a quasineutral equation for the electric potential

$$\phi_1 = q_1/p_0, \quad p_0 = n_{c0}/t_{c0} - n_{i0}/v_{i0}^2 - n_{e0}/v_{e0}^2,$$
$$q_1 = n_{i0}(j_{i1}/j_{i0} - k_{i1}/v_{i0}^2) - n_{e0} j_{e1}/j_{e0}, \tag{32}$$

and the dynamic equations for ions

$$\frac{dj_{i1}}{d\xi} - \frac{i\omega}{v_{i0}}\left(j_{i1} - j_{i0}\frac{k_{i1}-\phi_1}{v_{i0}^2}\right) = 0,$$
$$\frac{dk_{i1}}{d\xi} - \frac{i\omega}{v_{i0}}(k_{i1}-\phi_1) = 0. \tag{33}$$

Once ϕ_1 is substituted, the general solution of Eq. (33), is combination of two ion–acoustic modes (which are the solution of the homogeneous problem) and a standing mode, proportional to j_{e1}.

Four boundary conditions have already been imposed in Eq. (31) for the quasisteady electrons: j_{e1} and k_{e1} are constant across the DL; zero flow of species c across the DL; n_{c1} and ϕ_1 verify the Boltzmann equilibrium equation. Three boundary conditions are still needed to close the problem. The first one is the Langmuir condition (4), which, with the help of the rest of DL jump conditions, becomes

$$(v_{i0D}^- - v_{i0D}^+)\left(\frac{j_{i1D}^-}{j_{i0}} + \frac{i\omega\xi_{D1}}{v_{i0D}^-} - \frac{2\xi_{D1}}{\xi_{D0}} - \frac{k_{i1D}^- + i\omega\xi_{D1}v_{i0D}^-}{v_{i0D}^+ v_{i0D}^-}\right)$$
$$= (v_{e0D}^- - 2v_{e0D}^+)\frac{j_{e0}}{j_{i0}}\left(\frac{j_{e1}}{j_{e0}} - \frac{2\xi_{D1}}{\xi_{D0}}\right), \tag{34}$$

with superscripts + and − naming each of the DL sides. Finally, two boundary conditions on species i are imposed at $\xi=1$. For $p_0(1)=0$, one imposes the perturbation of the ion flow and the boundedness of ϕ_1, Eq. (32):

$$j_{i1}(1) = j_{i1R}, \quad q_1(1) = 0. \tag{35}$$

[For $p_0(1)>0$, $j_{i1}(1)=j_{i1R}$ and $k_{i1}(1)=k_{i1R}$ are specified.]

Since the core is assumed quasineutral, $\phi_1(1)$ is determined from Eq. (32)

$$\phi_1(1) \equiv \phi_{1N} = \lim_{\xi\to 1} q_1/p_0.$$

If the perturbation of ϕ_1 at the contactor surface wants to be fixed, say ϕ_{1R}, and differs from ϕ_{1N}, the Appendix shows that a small space-charge layer is formed, between the contactor at the quasineutral core, to adjust both values of ϕ_1. According to Eqs. (21) and (22), in the zero-Debye-length limit, $j_{\alpha 1}$ and $k_{\alpha 1}$ are invariant across that layer, but $n_{\alpha 1}$ and $v_{\alpha 1}$ change with ϕ_1.

The practical procedure to solve core equations is the following: First, the presheath solution provides ξ_{D1}/j_{e1}; second, Eq. (34) yields k_{i1D}^- as linear combination of j_{e1} and j_{i1D}^-; third, the integration of Eq. (33) from $\xi=\xi_{D0}^-$ to $\xi=1$ yields the solution of the core in terms of these two flow parameters [this numerical integration does not pose any difficulty once the equations are made regular around $\xi=1$ in a way similar to the presheath]; and fourth, imposing the two conditions (35) at $\xi=1$, one has

$$[j_{i1D}^- \;\; j_{e1}]A = j_{i1R}B,$$

with A and B matrices of sizes 2×2 and 1×2, respectively, which determines completely the perturbation response in terms of j_{i1R} and ω.

Temporal eigenmodes of a particular steady solution (characterized by j_{i0}, ϕ_{0R}, and t_{c0}) correspond to a nonzero response to $j_{i1R}=0$, so they are the solutions of the global dispersion equation

$$D(\omega; j_{i0}, \phi_{0R}, t_{c0}) \equiv \det A = 0. \tag{36}$$

Unstable solutions correspond to eigenmodes with $\omega_{im}>0$.

A. Asymptotic analysis for $|\omega| \gg 1$

Before computed results are discussed, an asymptotic solution of the perturbation response for large ion frequencies is presented. The aim of this analysis is threefold: First, to get a better understanding of the different plasma modes that are launched in the two plasma regions and their interaction; second, to obtain asymptotic scaling laws for the variation of the main plasma parameters; and third, to have an alternative integration method for $|\omega| \gg 1$, when the preceding numerical scheme becomes slow and unreliable.

The asymptotic solution of presheath equation (27) for $|\omega_a \xi_{D0}| \gg 1$ is the combination of the WKB (Wentzel–Kramers–Brillouin) solution[14] of the homogeneous problem plus a particular solution proportional to j_{e1}

$$j_{a1}(\xi) \simeq \tilde{a}_\infty \alpha_p(\xi)\exp[-\beta_p(\xi)] + j_{e1}\frac{4iv_{e0}}{\omega_a \xi}\frac{1+3t_{e0}}{1+3t_{e0}-v_{e0}^2},$$
$$j_{e0}k_{a1}(\xi) \simeq -\frac{\tilde{a}_\infty}{\alpha_p(\xi)}\exp[-\beta_p(\xi)] + j_{e1}v_{e0}^2, \tag{37}$$

with

$$\alpha_p(\xi) = (1+3t_{e0}-v_{e0}^2)^{-1/4} v_{e0}^{-1/2},$$
$$\beta_p(\xi) = -i\omega_a \int_{\xi_{D0}^+}^{\xi} (1+3t_{e0}-v_{e0}^2)^{-1/2} d\xi,$$

and $\tilde{a}_\infty$ a constant — proportional to a_∞ in Eq. (28). The expression of β_p shows that the WKB mode is an ion–electron mode traveling outwards with (dimensionless) local, group velocity $\sqrt{1+3t_{e0}-v_{e0}^2}$.

Close to ξ_{D0}^+ it is

$$1+3t_{e0}-v_{e0}^2 \simeq a_0(\xi/\xi_{D0}-1)^{1/2},$$

with $a_0 = -2^{3/2}(v_{e0D}^+\sqrt{2(v_{e0D}^+)^2-1})$, so the presheath/DL boundary is a singular point of the WKB solution. For $\xi/\xi_{D0}-1 \ll 1$, the solution that matches with (37) is

$$j_{a1}(\xi) \simeq \begin{cases} \tilde{a}_\infty c_1(\mathrm{Ai}(z)+i\mathrm{Bi}(z)) + j_{e1}c_2\mathrm{Hi}(z), & (\omega_{\mathrm{im}}=0), \\ 2i\tilde{a}_\infty c_1 \mathrm{Ai}(z) - j_{e1}c_2\mathrm{Gi}(z), & (\omega_{\mathrm{im}}\neq 0), \end{cases}$$

where Ai, Bi, Gi, and Hi are Airy functions,[15] and

$$z(\xi) = \frac{(2\omega_a\xi_{D0})^{2/3}}{a_0^{1/3}}\left(\frac{\xi}{\xi_{D0}}-1\right)^{1/2},$$
$$c_1 = \frac{\sqrt{\pi}(2\omega_a\xi_{D0})^{1/6}}{|v_{e0D}^+|^{1/2}a_0^{1/3}i^{1/2}}, \quad c_2 = \frac{8\pi i(v_{e0D}^+)^3}{a_0^{4/3}(2\omega_a\xi_{D0})^{1/3}};$$

the expressions for $k_{a1}(\xi)$ are omitted. Boundary conditions (29) and (30) at $\xi=\xi_{D0}^{+}$ relate $\tilde{a}_\infty$ and j_{e1} to ξ_{D1}. Keeping only the dominant terms, one has

$$\frac{j_{e1}}{j_{e0}} \simeq \frac{\sqrt{3}}{8\pi} \frac{(2a_0\omega_a\xi_{D0})^{4/3}}{4\mathrm{Ai}(0)(v_{e0D}^{+})^4} \frac{\xi_{D1}}{\xi_{D0}},$$
$$\frac{\tilde{a}_\infty}{j_{e0}} \simeq c_3 \frac{\mathrm{i}(2\omega_a\xi_{D0})^{5/6}a_0^{1/3}}{8\mathrm{Ai}(0)|\pi v_{e0D}^{+}|^{1/2}} \frac{\xi_{D1}}{\xi_{D0}}, \tag{38}$$

with c_3 equal to 1 and $2\mathrm{i}^{1/2}$, for $\omega_{im}\neq 0$ and $\omega_{im}=0$, respectively.

In the core, the asymptotic solution of Eq. (33), for $|\omega| \gg 1$, is the combination of two WKB modes plus the particular solution proportional to j_{e1}

$$j_{i1}(\xi)=\alpha[C_+\exp(-\beta_+)+C_-\exp(-\beta_-)] + O(j_{e1}\omega^{-1}),$$
$$k_{i1}(\xi)=\frac{1}{j_{i0}\alpha}[C_+\exp(-\beta_+)-C_-\exp(-\beta_-)] - \frac{n_{e0}}{n_{c0}/t_{c0}-n_{e0}/v_{e0}^2}\frac{j_{e1}}{j_{e0}}, \tag{39}$$

with

$$\alpha(\xi)=\left[\frac{1}{v_{i0}^2 n_{i0}}\left(\frac{n_{c0}}{t_{c0}}-\frac{n_{e0}}{v_{e0}^2}\right)\right]^{1/4},$$
$$\beta_\pm(\xi)=-\mathrm{i}\omega\int_1^\xi \frac{d\xi}{v_{i0}\pm[(t_{c0}n_{i0})/(n_{c0}-n_{e0}t_{c0}/v_{e0}^2)]^{1/2}}.$$

The expression for $\beta_\pm$ says that the two WKB modes are mounted on the out-streaming ion beam and travel in opposite directions with a sound speed that depends weakly on v_{e0}. Imposing boundary condition (35) at $\xi=1$, one has

$$C_-=0,\ C_+=v_{i0R}^2 j_{i1R},$$

so there is no mode traveling inwards from the ion beam. [For $p_0(1)>0$, both ion–acoustic modes are generally present.] Finally, the relation between j_{e1} and j_{i1R} is obtained from Langmuir condition (34); for $|\omega|\gg 1$ this reduces to

$$j_{e1}v_{e0D}^{-}/v_{i0D}^{+}-\mathrm{i}\omega\xi_{D1}j_{i0}/v_{i0D}^{-}+o(\omega\xi_{D1})\simeq j_{i1D}^{-}. \tag{40}$$

VI. RESULTS

A. Dynamic response to perturbations in plasma emission

Figure 3 shows the spatial-temporal response of the electric potential, $\Phi(r,t)=\Phi_0(r)+\Phi_1(r,t)$, for two different oscillation modes on $J_i(R,t)$. Nonlinear perturbation terms are not included, so large perturbations in the plots are intended only to stand out the salient features of the plasma response. The precedent analysis has shown that a perturbation J_{i1R} is transmitted along the core by an outward, acoustic mode mounted on the beam of emitted ions. Its (local) group velocity in the laboratory frame is

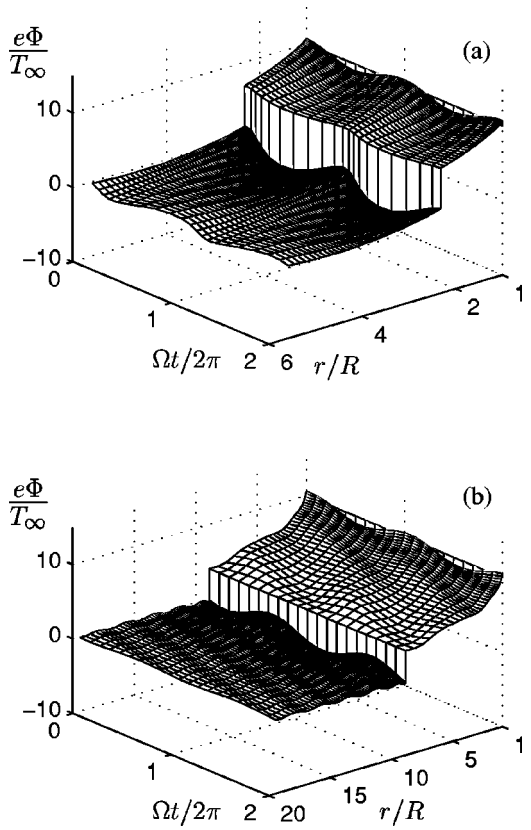

FIG. 3. Evolution of the electric potential for two oscillatory perturbations on the plasma emission: (a) $\omega=1.5$, $j_{i1R}/j_{i0}=0.2$, $j_{i0}=9.1$, $\phi_{0R}=10$, and $t_{c0}=1$; (b) $\omega=3$, $j_{i1R}/j_{i0}=0.2$, $j_{i0}=164.6$, $\phi_{0R}=10$, and $t_{c0}=1$. The displacement of the DL in (b) is imperceptible: $r_{D1}/r_{D0}<0.15\%$.

$$V_{i0}+\left[\frac{T_{c0}}{m_i}\left(\frac{1+N_{e0}/N_{c0}}{1-(N_{e0}/N_{c0})(T_{c0}/m_eV_{e0}^2)}\right)\right]^{1/2} \tag{41}$$

and the dependence on *e*-beam parameters indicates that the three species are interacting. When this ion–electron mode reaches the DL, it perturbs the pressure balance at the DL, which results in a perturbation of the flow of incoming electrons and a DL displacement, according to Langmuir and (singular) Bohm conditions. The perturbation on J_{e1} is transmitted as a standing mode to both core and presheath. The DL displacement r_{D1} excites another acoustic mode on the ambient ions that travels outwards with (local) group velocity $\sqrt{(T_\infty+3T_{e0})/m_a-V_{e0}^2}$. [The first, ion–acoustic mode, created at the contactor surface also travels through the presheath, but it is weak there, for the parametric range we are considering. For a supersonic ion emission, $P_0(R)>0$, one more ion–acoustic mode exists in the core.] The two plots of Fig. 3 illustrate that the acoustic modes dominate over the standing one as the frequency increases, and the displacement of the DL is smaller as the frequency and the core size increase.

The discontinuity observed in Fig. 3 at $r=R$ is the small space-charge layer that adjusts the dynamic response of Φ at the inner boundary of the quasineutral core, $r=R^+$ say, to a given value at the contactor surface, $r=R$. The physical relevance of that layer is uncertain since the transition from the internal (keeper and hollow cathode) regions of the contactor

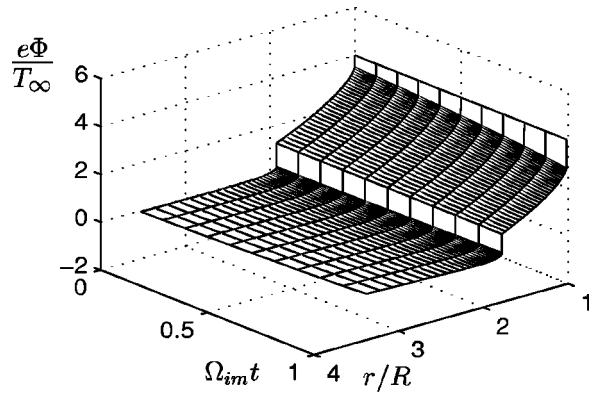

FIG. 4. Evolution of the electric potential for a monotonic plasma emission: $\omega=0.4i$, $\phi_{0R}=4$, $j_{i0}=12.3$, and $t_{c0}=1$.

to the external ones has not been modeled; furthermore, whether the current or the potential bias can be externally fixed depends on the characteristics of the whole electrical circuit.

Figure 4 shows the effect of a monotonic perturbation ($\omega_{\rm re}=0$, $\omega_{im}>0$) on $J_i(R,t)$ for the same steady solution that Fig. 3. A response with acoustic delay substitutes here the above wave-like behavior. Otherwise, the interactions among the different species and regions are similar. The retreat of the DL produces a small potential well at $r=r_{D0}^{+}$, not clearly seen in Fig. 4.

Figure 5(a) shows the temporal envelope [the dependence on $\exp(-i\Omega t)$ is omitted] of the spatial perturbation on $\hat{\phi}_1$ for $j_{i1R}\neq 0$ and different (real) frequencies. Figures 5(b) and 5(c) depict the evolution of parameters j_{e1} and ξ_{D1} with the oscillation frequency. For $\omega\gg 1$, these plots agree with the asymptotic laws obtained from Eqs. (38)–(40)

$$\xi_{D1}/\xi_{D0}\sim(\omega_a\xi_{D0})^{-4/3}j_{e1}/j_{e0}, \tag{42}$$

$$|j_{i1D}^{-}|\simeq|j_{i1R}|v_{i0R}^{2}\alpha(\xi_{D0}^{-}), \tag{43}$$

$$|j_{e1}|\simeq|j_{i1D}^{-}|. \tag{44}$$

Equation (42) is Bohm condition at the presheath/DL boundary. The strong decay of the relative DL displacement at high frequencies is due to the rigidity of the ambient ions in the presheath side, which constrains the DL mobility. This also explains the quasisteady form of Langmuir condition (44). The decay of j_{i1} from the contactor surface to the DL, Eq. (43), is due to the inhomogeneity of the steady spatial profile.

Figure 6 is similar to Fig. 5 but for purely monotonic modes. The main novelty here is that the region affected by the perturbation of j_{i1R} decreases with $\omega\gg 1$ due to the acoustic delay; this makes j_{e1}/j_{i1R} to decrease. For $\omega\gg 1$ the typical thickness of the region affected by a perturbation at the contactor is $\Delta r\sim\Omega^{-1}\sqrt{T_{c0}/m_i}$.

Figure 7 illustrates, for oscillatory modes, the evolution of the parameters of the perturbation response with the parameters of the steady solution. We again observe that the inhomogeneity of the steady solution in the core leads to a smaller dynamic response when ξ_{D0}^{-1}, ϕ_{0R}, or t_{c0} are smaller.

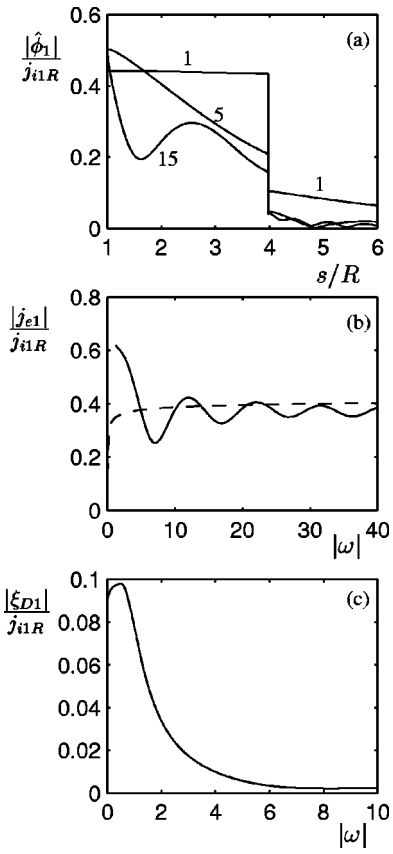

FIG. 5. Response to oscillatory perturbations ($\omega_{im}=0$) on the plasma emission ($j_{i1R}\neq 0$) for $\phi_{0R}=500$, $j_{i0}=21.6$, and $t_{c0}=10$. (a) Temporal envelope of the spatial profile of $\tilde{\phi}_1(s)$ for three values of $\omega(=1,\ 5,\ 15)$. (b) and (c) Perturbation of the electron current and DL displacement, as function of the ω-mode; the dashed line corresponds to the WKB-type solution, valid for $\omega\gg 1$.

B. On the radial, ion–electron instability

Numerical solving of dispersion equation [Eq. (36)] shows that it has no solution with $\omega_{im}>0$, within the range of validity of the steady solution. This result is confirmed by the asymptotic analysis for $|\omega|\gg 1$: Setting $j_{i1R}=0$ in Eq. (40) the dispersion relation becomes

$$v_{e0D}^{-}v_{i0D}^{-}/v_{i0D}^{+}\simeq ij_{i0}\omega\xi_{D1}/j_{e1}.$$

This has no solution with $|\omega|\gg 1$, since, from Eq. (42), the right-hand side is of order $(\omega\xi_{D0})^{-1/3}$. Therefore, the core/DL/presheath structure does not present a radial, ion–electron (macro)instability.

This conclusion refutes the analyses of Refs. 6–8, which assert the generation, in the core, of the Buneman (macro)instability, together with an ion–acoustic (micro)instability. Both are two particular cases of the ion–electron instability in a two-species plasma. However, the plasma in the core consists of three species and supports only one pair of ion–electron modes, with the ions interacting simultaneously with the two electron species, as Eq. (41) shows. The local dispersion relation of the plasma (valid for short wavelengths) yields that an ion–electron (macro)instability develops if

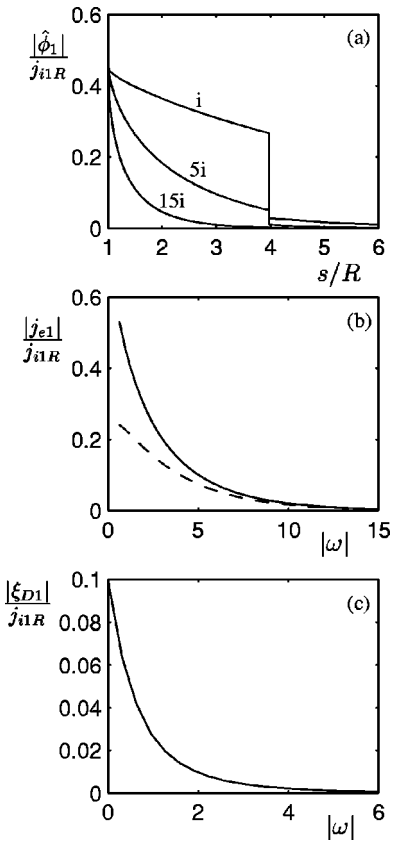

FIG. 6. Same as Fig. 5 but for plasma emissions monotonic with time. In (a) $\omega=1\mathrm{i},\ 5\mathrm{i},\ 15\mathrm{i}$; in (b) and (c) $|\omega|=|\omega_{im}|$.

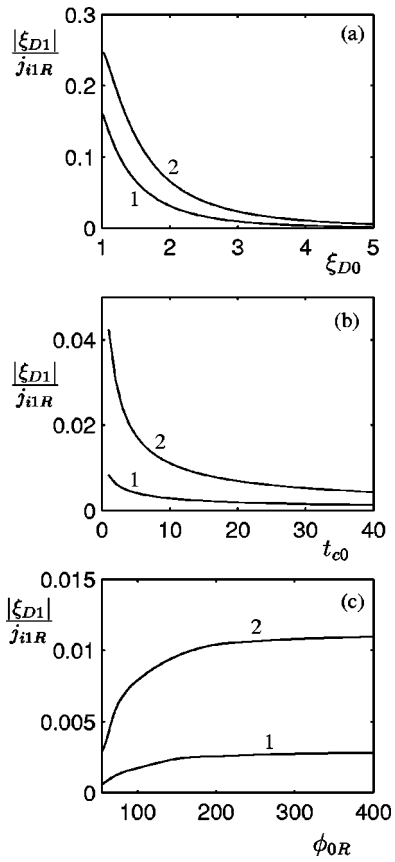

FIG. 7. Influence of the different steady solution parameters on the DL displacement for two perturbation modes on the plasma emission: $\omega=3.16(1)$ and $3.16\mathrm{i}(2)$. In (a) $\phi_{0R}=500$ and $t_{c0}=10$; in (b) $\phi_{0R}/t_{c0}=50$ and $\phi_{0D}/t_{c0}=46$; in (c) $t_{c0}=10$ and $\xi_{D0}=3.98$; ξ_{D0} is used as independent parameter instead of j_{i0}.

$$3T_{e0}<m_eV_{e0}^2<3T_{e0}+T_{c0}N_{e0}/N_{c0}, \tag{45}$$

(for $T_{i0}\ll T_{c0}$). When $N_{c0}=0$, this expression recovers the well-known instability range for a two-species plasma; but, when $N_{e0}/N_{c0}\leqslant O(1)$, the instability interval is narrow and does not include the Buneman limit. In the core, one has $N_{e0}/N_{c0}<1$ and $|V_{e0}|\gg\sqrt{3T_{e0}/m_e}$, typically, so there is no ion–electron macroinstability. The physical interpretation of Eq. (45) is the following: *c*-species has a stabilizing effect always, while the *e*-beam is de-stabilizing for $m_eV_{e0}^2>3T_{e0}$; N_{e1} and N_{c1} have opposite signs in this velocity range; the combined effect of the two beams is de-stabilizing when $N_{e1}>N_{c1}$, which justifies the upper-bound of Eq. (45).

For the range $e\Phi_{0R}/T_\infty\gg1$ considered here, one has $N_{i1}/N_{e1}\sim N_{i0}/N_{e0}\sim\sqrt{e\Phi_{0R}/T_\infty}$ in the presheath, and the influence of the *i*-beam on the regular, dynamic response of the presheath is negligible. Nevertheless, the weak *i*-beam could still launch an ion–electron macroinstability there. The interaction of the *i*-beam with the ambient electrons generates two additional ion–acoustic modes in the presheath. It turns out that one of them is *locally* unstable, but only in the region, close to the DL, where $3T_{e0}<m_eV_{e0}^2<T_\infty+3T_{e0}$. [In fact, experimentally detected fluctuations in that region[4,5] could be due to this behavior.] We have investigated the nonlocal influence of these modes for $\omega\gg1$ (and $e\Phi_{0R}/T_\infty\gg1$). The two new modes were added to the asymptotic solution of the presheath, and the core/presheath coupling was appropriately modified. The resulting dispersion relation still does not detect an ion–electron (macro)instability. It would be interesting to analyze the case when $e\Phi_{0R}/T_\infty$ is not too large, but then the *i*-beam modifies also the steady solution of the presheath, a case not completed yet.

The model derived here does not include collisions with the ejected gas in the plasma plume, which seem important in actual laboratory experiments. The main effect of electron–neutral collisions would be additional ionization in the core, which certainly modifies the flow and density of ions, but Ahedo[13] showed that the electron beam was affected weakly. Since according to our analysis, the ion–electron instability depends on condition (45) on the electron beam, it is plausible that external ionization has no significant role in the instability generation. Furthermore, if V_{i0} has any part on it, external ionization should have an stabilizing effect since it reduces the average ion velocity.

VII. FINAL CONSIDERATIONS

We first summarize the most salient features of the preceding analysis. The dynamic response of the core/DL/presheath structure is the combination of a quasisteady electron mode and several ion–electron modes, with different propagation characteristics in core and presheath. These two regions interact through the DL, which is itself displaced. The time-dependent behavior of the DL is determined by Langmuir law on dynamic pressure balance, Bohm law on

the plasma flow, continuity conditions on the flows of the free species, and barrier conditions on confined species. Indeed, at large frequencies ambient ions tend to be rigid, and the barrier effect restricts the DL displacement. Notice that the analysis of the time-dependent conditions at the DL is valid independently of the particular configuration of the quasineutral plasmas outside the DL; in particular it is valid for DL structures created in triple-plasma chambers. Our analytical model has also allowed a careful study of boundary conditions at the ambient plasma and the contactor surface, avoiding one of the main problems of numerical simulations.

The main conclusion of the stability analysis is the nonexistence of any radial, ion–electron macroinstability of the global plasma structure, including the Buneman instability, proposed by several authors. The ion–acoustic (micro)instability, due to Landau kinetic effect, could not be studied with the present, macroscopic model. The classical theory[9] states that the interaction of the supersonic *i*-beam with *c*-electrons generates locally unstable modes in the core. A first issue to investigate is how the presence of the *e*-beam modifies them: It is already known that the (real part of the) phase velocity is affected. If the *local* modes are still unstable, the next issue would be to find the way to include them into the dynamic behavior of the *global* plasma structure.

Two extensions of the dynamic analysis initiated here are now in progress. The first one is the investigation of the electron range of frequencies, when the plasma response is determined by electron–acoustic modes and a rigid background of ions. An unstable behavior of the plasma structure is more likely in that range, since unstable modes are detected by the local dispersion relation; the experimental data of Vannaroni *et al.*[2] supports also this idea. The second extension is to analyze the oblique (or nonradial) dynamic response, and the existence of an oblique, ion–electron instability. In a previous paper[16] we already derived an oblique, stationary model, expanding spatial perturbations in the full set of spherical harmonics, but ignoring temporal perturbations, i.e., we took $\Omega=0$. The analysis of the oblique, stationary modes detected that some of them were unstable. Presumably they represent the zero-frequency limit of the oblique, ion–electron instability.

ACKNOWLEDGMENTS

This research was supported by Ministerio de Educación y Cultura of Spain under Project PB97-0574-C04-02.

APPENDIX: PERTURBATION SHEATH AT THE CONTACTOR SURFACE

Equations (31)–(33) for the core determine the value of the perturbation potential at the inner boundary of the quasineutral core,

$$\phi_1(1^+)=\lim_{\xi=1^+} q_1/p_0=\phi_{1N}.$$

If the potential at the contactor surface ϕ_{1R} is imposed and it differs from ϕ_{1N}, a boundary, space-charge layer is needed to adjust these two values. Within this layer, Eq. (32) is substituted by quasiplanar Poisson equation

$$\epsilon^2 d^2\phi_1/d\xi^2=p_0\phi_1-q_1, \tag{A1}$$

with $\epsilon=\lambda_{D\infty}/R\ll 1$. The characteristic thickness of the boundary layer depends on $p_0(1)$. For the regular case $p_0(1)>0$, the expansion of p_0 and q_1 in Eq. (A1) yields

$$p_0\phi_1-q_1=p_0(1)(\phi_1-\phi_{1N})+O(\xi-1),$$

where we took into account that $j_{i1}=j_{i1}(1)+O(\xi-1)$, $k_{i1}=k_{i1}(1)+O(\xi-1)$. Using $\eta=\sqrt{p_0(1)}(\xi-1)/\epsilon$ as the layer spatial variable and taking $\epsilon\to 0$, Eq. (A1) becomes $d^2\phi_1/d\eta^2=\phi_1-\phi_{1N}$. The solution that verifies boundary conditions

$$\phi_1|_{\eta=0}=\phi_{1R},\quad \phi_1|_{\eta=+\infty}=\phi_{1N}, \tag{A2}$$

is $\phi_1(\eta)\simeq\phi_{1N}+(\phi_{1R}-\phi_{1N})\exp(-\eta)$.

For the singular case $p_0(1)=0$, the expansion of the right-hand side of Eq. (A1) is

$$p_0\phi_1-q_1=a(\phi_1-\phi_{1N})(\xi-1)^{1/2}+O(\xi-1),$$

with $a=2\sqrt{q_0(dp_0/d\phi_0)|_{\xi=1}}$, and the appropriate layer variable now is $\eta=a^{2/5}(\xi-1)/\epsilon^{4/5}$, which, for $\epsilon\to 0$, transforms Eq. (A1) into $d^2\phi_1/d\eta^2=(\phi_1-\phi_{1N})\eta^{1/2}$, and condition (A2) still apply. The solution to this problem is

$$\phi_1(\eta)\simeq\phi_{1N}+\frac{2^{7/5}}{5^{2/5}}\frac{\phi_{1R}-\phi_{1N}}{\Gamma(2/5)}\eta^{1/2}K_{2/5}\left(\frac{4}{5}\eta^{5/4}\right),$$

where $\Gamma(x)$ is the Gamma function and $K_{2/5}$ the modified Bessel function[15] that satisfies $K_{2/5}(x)\sim e^{-x}\sqrt{\pi/2x}$ for $x\gg 1$.

Therefore, the thickness of the space-charge layer is $\Delta\xi\sim\epsilon$ and $\Delta\xi\sim\epsilon^{4/5}$ (i.e., $\Delta r\sim\lambda_{D\infty}$ and $\Delta r\sim\lambda_{D\infty}^{4/5}R^{1/5}$) for the regular and singular cases, respectively. In both situations and for $\epsilon\to 0$, j_{i1} and k_{i1} are constant in the boundary layer but not $v_{\alpha 1}$ and $n_{\alpha 1}$, which depend on ϕ_1, Eq. (22).

[1] J. Williams and P. J. Wilbur, J. Spacecr. Rockets **27**, 634 (1990).
[2] G. Vannaroni, M. Dobrowolny, E. Melchioni, F. de Venuto, and R. Giovi, J. Appl. Phys. **71**, 4709 (1992).
[3] L. Conde and L. León, Phys. Plasmas **1**, 2441 (1994).
[4] N. Hershkowitz, Space Sci. Rev. **41**, 351 (1985).
[5] M. A. Raadu, Phys. Rep. **178**, 26 (1989).
[6] D. Hastings and N. Gatsonis, Acta Astron. **17**, 827 (1988).
[7] L. Iess and M. Dobrowolny, Phys. Fluids B **1**, 1880 (1989).
[8] A. Gioulekas and D. Hastings, J. Propul. Power **6**, 559 (1990).
[9] N. A. Krall and A. Trivelpiece, *Principles of Plasma Physics* (San Francisco Press, San Francisco, CA, 1986).
[10] H. Marshall and F. M. Neubauer, *Proceedings of the 4th International Conference on Tethers in Space, Washington D.C. 1995* (Science and Technology Corporation, 101 Research Drive, Hampton, VA 23666-1340, 1995), p. 1009.
[11] G. Joyce and R. Hubbard, J. Plasma Phys. **20**, 391 (1978).
[12] E. Ahedo, J. Sanmartín, and M. Martínez-Sánchez, Phys. Fluids B **4**, 3847 (1992).
[13] E. Ahedo, Phys. Plasmas **3**, 3875 (1996).
[14] C. M. Bender and S. A. Orszag, *Advanced Mathematical Methods for Scientists and Engineers* (McGraw-Hill, Singapore, 1986), p. 484.
[15] M. Abramowitz and I. Stegun, *Handbook of Mathematical Functions* (Dover, New York, 1965).
[16] E. Ahedo and V. Lapuerta, Phys. Plasmas **2**, 3252 (1995).